

1-1-2012

## Characterization of a total power radiometer

MURAT CELEP

ŞENEL YARAN

YAKUP GÜLMEZ

ARİF DOLMA

Follow this and additional works at: <https://journals.tubitak.gov.tr/elektrik>



Part of the [Computer Engineering Commons](#), [Computer Sciences Commons](#), and the [Electrical and Computer Engineering Commons](#)

---

### Recommended Citation

CELEP, MURAT; YARAN, ŞENEL; GÜLMEZ, YAKUP; and DOLMA, ARİF (2012) "Characterization of a total power radiometer," *Turkish Journal of Electrical Engineering and Computer Sciences*: Vol. 20: No. 6, Article 4. <https://doi.org/10.3906/elk-1010-847>

Available at: <https://journals.tubitak.gov.tr/elektrik/vol20/iss6/4>

This Article is brought to you for free and open access by TÜBİTAK Academic Journals. It has been accepted for inclusion in Turkish Journal of Electrical Engineering and Computer Sciences by an authorized editor of TÜBİTAK Academic Journals. For more information, please contact [academic.publications@tubitak.gov.tr](mailto:academic.publications@tubitak.gov.tr).

# Characterization of a total power radiometer

Murat CELEP<sup>1,\*</sup>, Şenel YARAN<sup>1</sup>, Yakup GÜLMEZ<sup>1</sup>, Arif DOLMA<sup>2</sup>

<sup>1</sup>*Technological and Scientific Research Council of Turkey, National Metrology Institute, Gebze, Kocaeli-TURKEY*

*e-mail: murat.celep@ume.tubitak.gov.tr*

<sup>2</sup>*Department of Electronics and Communication Engineering, Kocaeli University, Kocaeli-TURKEY*

Received: 21.10.2010

## Abstract

*The performance parameters of a total power radiometer designed as a noise measurement system for the frequency range of 12-18 GHz were investigated. The total power radiometer included a low-noise radio frequency section, a narrow-band intermediate frequency section, an average power detector, and a symmetric microwave switch. The radiometer's stability versus time was  $0.343 \times 10^{-5}$  mW/h and its stability against temperature fluctuation was 0.0035 mW/K. The temperature fluctuation of the radiometer was less than 4 mK. We proved that there was no need for active temperature control to obtain stable radiometer gain.*

**Key Words:** *Microwave noise, noise measurement, total power radiometer, calibration*

## 1. Introduction

Einstein, in his work on Brownian motion in 1905, predicted that the random motion of molecules in a liquid impacting on larger suspended particles would result in random motion of the particles [1]. In 1928, J.B. Johnson predicted that a similar random motion of electric charge due to thermal agitation existed in all conductors and produced random variation of the potential between the ends of a conductor. Johnson measured the effect of these fluctuations of electric charge in a conductor using an amplifier [2]. He called the effect noise, and it is now known as Johnson noise. To support Johnson's results, Nyquist theoretically described the effects of thermal agitation of electric charge in conductors [3]. Dicke predicted in 1946 that there was a connection between Johnson noise and thermal radiation, and he compared the radiation from an antenna with that generated by a reference resistor using a radiometer [4]. This measurement system, based on a reference resistor, is now known as the Dicke radiometer and is commonly used to measure microwave noise.

Several metrology institutes began to use modified Dicke radiometers in the 1960s to measure microwave noise standards. In 1960, Estlin et al., from the National Bureau of Standards in the United States, now the National Institute of Standards and Technologies (NIST), used a modified Dicke radiometer for microwave noise

---

\*Corresponding author: Technological and Scientific Research Council of Turkey, National Metrology Institute, Gebze, Kocaeli-TURKEY

source calibration [5]. A description of this microwave noise source calibration system was reported by Wells et al., at the same institute, in 1964 [6]. In 1968, Somlo and Hollyway of the National Standards Laboratory, Australia, reported a waveguide X-band radiometer for the calibration of primary-level noise sources [7]. In 1972, Blundell et al. used a radiometer to establish the microwave noise measurement standard of the Royal Radar Establishment, United Kingdom [8]. Although the Dicke radiometer has good gain stability, its sensitivity is insufficient for precise measurements. Therefore, a total power radiometer with better sensitivity and drift performance was sought [9] and [10]. Nowadays, total power radiometers are used in a wide range of metrological research applications.

In this article, the performance and the uncertainty of a coaxial-type total power radiometer developed at the National Metrology Institute of Turkey (UME) is investigated, and the uncertainty of the total power radiometer is reported to be 0.17-0.30 dB ( $k = 2$ , level of confidence 95%).

## 2. Theory of the total power radiometer

The total power radiometer shown in Figure 1 is a superheterodyne receiver [11] that consists of 3 main parts: a radio frequency (RF) section, an intermediate frequency (IF) section, and an average power detector [12]. The RF section amplifies and filters the low-level, wideband noise signal applied to the radiometer input. The available power of the noise signal,  $P_{av}$ , is given by:

$$P_{av} = k T B, \quad (1)$$

where  $k$ ,  $T$ , and  $B$  are the Boltzmann constant ( $1.38 \times 10^{-23}$  J/K), noise temperature (K), and system noise bandwidth (Hz), respectively. The applied noise signal has a wider bandwidth than the radiometer. The function of the RF amplifier is to filter and amplify the input signal with the bandwidth  $B_{RF}$ . The mixer downconverts RF signals to IF signals, and the IF amplifier provides further amplification to detectable levels. The system noise bandwidth  $B$  is determined by the filter in the IF section.

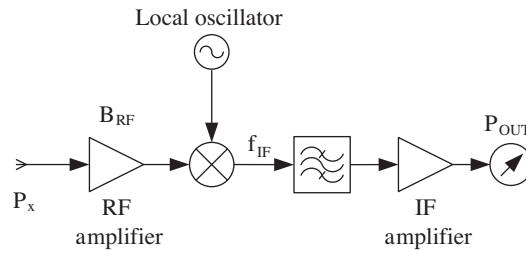


**Figure 1.** Block diagram of the total power radiometer.

Under ideal conditions, the applied input noise signal is amplified by an available gain  $G$  in system noise bandwidth  $B$  and is detected by the power detector. In practice, however, the radiometer also produces a noise signal at any temperature over absolute zero. This noise signal is added to the applied input noise signal. For simplicity, it is assumed that the radiometer is noise-free and that the internally generated noise power is applied to the radiometer input.

Therefore, the total noise power at the radiometer input,  $P_{IN}$ , is the sum of the noise signals from the noise source and from the radiometer, as given below:

$$P_{IN} = P_x + P_{Rad}, \quad (2)$$

where  $P_x$  and  $P_{Rad}$  are the available noise power applied to the input from the noise source and the noise power generated by the radiometer, respectively.

When a noise power  $P_x$  is applied to the radiometer input, a power  $P_{OUT}$  related to the sum of  $P_x$  and  $P_{Rad}$  is obtained at the radiometer output, as follows:

$$P_{OUT} = G k (T_x + T_{Rad}) B, \tag{3}$$

where  $G$ ,  $k$ ,  $T_x$ ,  $T_{Rad}$ , and  $B$  are the available gain, Boltzmann constant, the applied noise temperature, the radiometer noise temperature, and the system noise bandwidth, respectively.

The total power radiometer has a wide range of potential applications. In metrology, for example, total power radiometers are used for primary-level microwave noise measurements [13]. Standard, ambient, and unknown noise sources are connected to the radiometer input, and the respective output powers are measured. Generally, a microwave switch is used to connect several noise sources to the radiometer input so that the input noise source can be selected from among them without requiring reconnection.

An unknown noise source temperature,  $T_x$ , can be calculated using the following equation [14]:

$$T_x = T_a + (T_s - T_a) \frac{(Y_x - 1) M_s \eta_s}{(Y_s - 1) M_x \eta_x}, \tag{4}$$

noise temperature (K),  $Y_x$  is the ratio of output powers (unknown Y-factor) when the unknown and the ambient noise sources are alternately connected to the radiometer input,  $Y_s$  is the ratio of output powers (standard Y-factor) when the standard and the ambient noise sources are alternately connected to the radiometer input,  $M_x$  is the mismatch factor between the unknown noise source and the radiometer input,  $M_s$  is the mismatch factor between the standard noise source and the radiometer input, and  $\eta_x$  and  $\eta_s$  are the efficiencies of microwave switch paths connected to the unknown and the standard noise sources, respectively.

### 3. Developing and characterizing the radiometer

The coaxial total power radiometer, established for microwave noise measurements between 12 and 18 GHz, is shown in Figure 2. The radiometer is composed of a microwave switch, RF, IF, and detector sections. Standard, ambient, and unknown noise sources are selected in turn using the microwave switch. The noise signal applied to the input is amplified and filtered in the RF section. An RF amplifier with a low noise figure was chosen, because the initial components of the radiometer are predominant in the radiometer noise temperature [15,16]. The signal is downconverted to 30 MHz IF by employing a mixer in the RF section. In the IF section, the IF signal is filtered and amplified to reach a detectable level. In the IF section, an attenuator was used in order to operate the amplifiers in their linear region. In the detector section, the noise signal is detected by an averaging power sensor and read by a power meter.

The output power of a radiometer depends directly on the radiometer gain, as given in Eq. (3). Therefore, gain fluctuations cause changes in the output power level. There are 3 important parameters that affect the radiometer gain: voltage change in the power supply of the amplifiers and the noise sources, temperature fluctuation of the radiometer [17], and the measurement time. In order to obtain stable gain against voltage changes, a power supply with stability better than 50 ppm was designed at the UME. Instability of the power supply caused an error of less than 0.001 dB in excess noise ratio (ENR) values of noise sources, which is negligible in the total uncertainty. To obtain a stable gain against temperature fluctuation, the microwave

switch, RF section, and IF section were mounted on huge thermal blocks. Stability and linearity tests were performed to determine the performance of the radiometer.

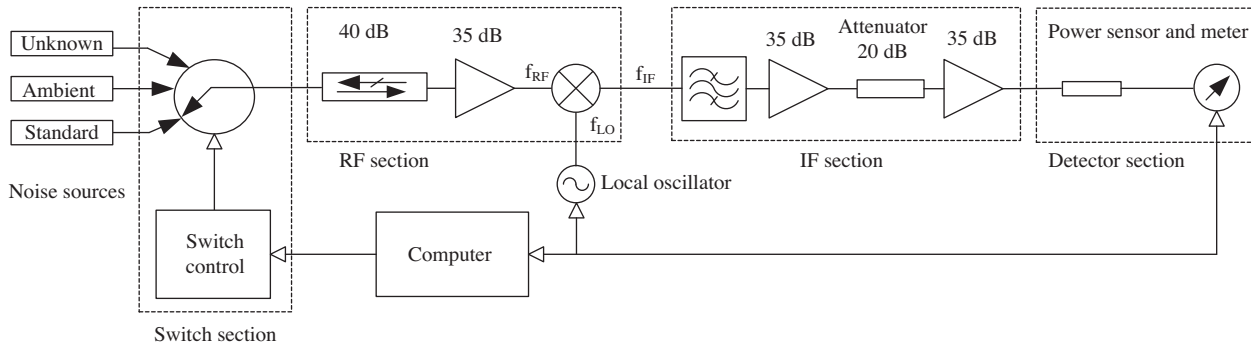


**Figure 2.** The configuration of the total power radiometer.

### 3.1. Stability tests

To determine the stability of the radiometer, a noise source with a nominal 5 dB ENR was connected to the radiometer input. The temperature dependence and long-term stability of the measurement system were investigated during the stability tests. The radiometer temperature dependence is shown in Figure 3.

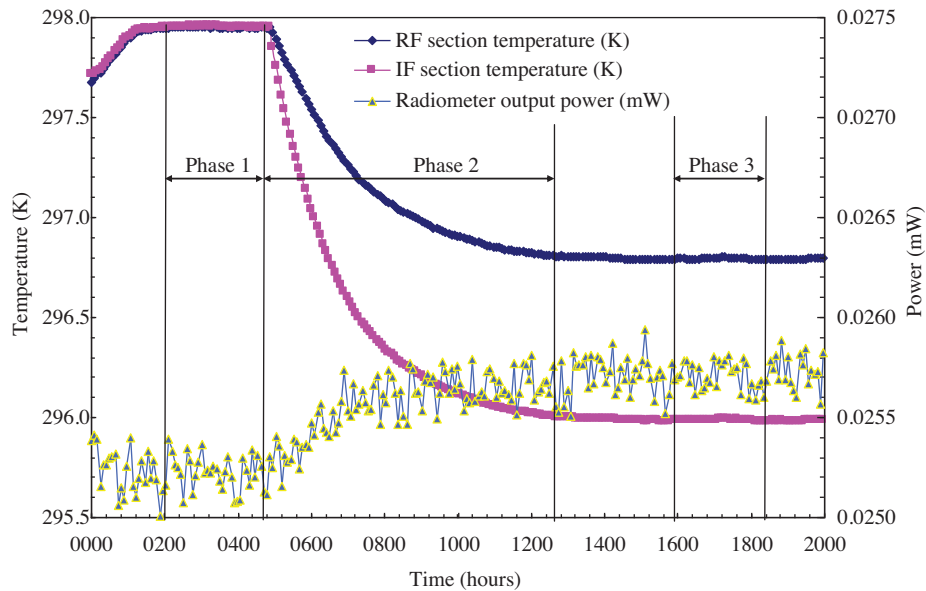


**Figure 3.** Radiometer response to temperature fluctuation.

The output power and temperatures of the IF and RF sections were measured simultaneously. For temperature measurements, precision negative temperature coefficient (NTC) resistors and multimeters were employed. Before the temperature measurements, all of the NTC resistors were calibrated for temperatures from 18 to 30 °C. To precisely monitor the temperature of the RF and IF sections, the NTC resistors were embedded in the center of the main blocks of the radiometer. A temperature-controlled water bath with 0.1-K stability was manufactured and used to maintain the stable temperatures of the RF and IF sections at a fixed level. The temperature dependence of the measurement system was analyzed in 3 phases. In the first

phase, the temperature of the system was maintained at 25 °C using the temperature-controlled water bath. At the beginning of the second phase, the temperature-controlled bath was deactivated. The second phase ended when thermal equilibrium was reached. In the third phase, all of the measurements were taken at the stable environmental temperature, without active temperature control. The temperature of the RF section was higher than the temperature of the IF section because of the relatively high thermal power of the RF amplifier. The standard deviations of the results throughout the 2.5 h of measurement time, with and without active temperature control, are given in Table 1.

**Table 1.** Standard deviations of the phase 1 and phase 3 results.

Stage	Standard deviations of temperatures (K)		Standard deviation of the output power (mW)
	For the RF section	For the IF section	
Phase 1	0.0034	0.0031	$8.73 \times 10^{-5}$
Phase 3	0.0035	0.0032	$6.77 \times 10^{-5}$

The radiometer’s response to the temperature fluctuation of the RF ( $\partial P_{out}/\partial T_{RF}$ ) and IF ( $\partial P_{out}/\partial T_{IF}$ ) sections was analyzed using the second phase results to determine its temperature dependence. Functions describing the output power versus the temperature of the RF and IF sections were defined using logarithmic fitting. The temperature coefficients of the RF and IF sections were calculated from these functions and found to be  $-0.00036$  mW/K for the RF section and  $-0.00024$  mW/K for the IF section.

The maximum output power deviation versus temperature fluctuation was calculated to be  $-1.26 \times 10^{-6}$  mW for the RF section in the third phase, using the temperature coefficients and temperature fluctuations of the RF and IF sections given in Table 1. This value is lower than the observed power deviation in the third phase. Therefore, the effects of the temperature fluctuations, even without active temperature control, should have a negligible effect on noise temperature measurements, primarily because of the huge copper blocks in the radiometer.

To determine the long-term stability of the output power, a noise source was measured every 3 min during the 5 h spent at the frequencies from 12 to 18 GHz with a 1 GHz step. A straight line was fitted to the output power level measurements at each frequency, and the slope of this line was calculated. The results for 18 GHz are shown in Figure 4. The largest drift was found to be  $1.43 \times 10^{-5}$  mW/h, which was accepted as the long-term-stability of the radiometer, and is negligible. The noise temperature measurement time was shortened to decrease the drift error and prevent the effects of instantaneous environmental temperature fluctuations.

### 3.2. Linearity tests

Standard, ambient, and unknown noise sources generally have different noise temperatures. Therefore, each applies a different level of noise power to the radiometer input. Thus, a linear response of the radiometer to different noise power levels is highly desirable. A waveguide below cut-off (WBCO) attenuator has traditionally been employed in the IF section to remove the linearity errors of the detector [18,19]. However, in this study, no WBCO attenuator was used, because of their high cost. The linearity test set-up constructed at the UME is shown in Figure 5. The set-up enables the linearity test to be performed at different noise powers.

To obtain an adjustable noise source, a 1 dB step attenuator was connected to a noise source with a nominal 15 dB ENR. The ENR values of the standard noise source and the noise source in the adjustable noise source module were certified by the National Physical Laboratory (NPL), United Kingdom, and the s-parameters of the step attenuator were measured using a vector network analyzer (VNA). The output noise

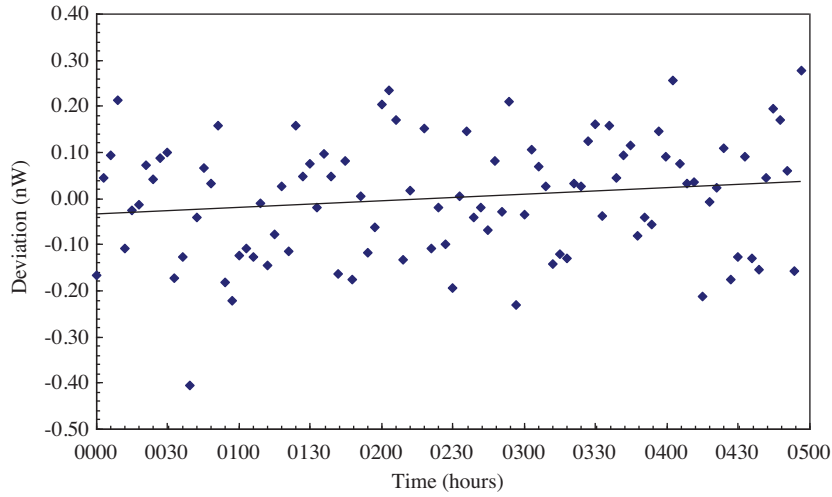


**Figure 4.** Long-term stability for 18 GHz.

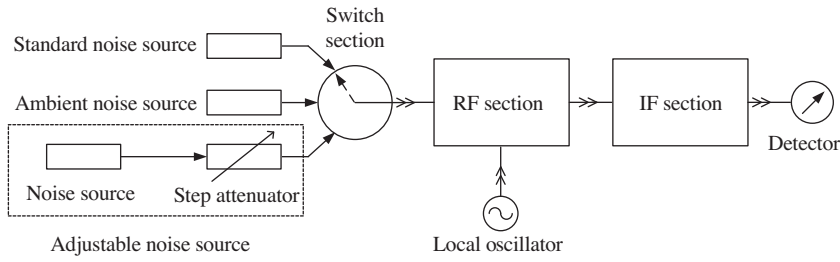


**Figure 5.** Linearity test set-up.

temperature of the adjustable noise source,  $T_u$ , was calculated using Eq. (5) [20].

$$T_u = T_d \alpha + T_a (1 - \alpha), \quad (5)$$

where  $T_d$  is the noise source noise temperature (K),  $T_a$  is the ambient temperature (K), and  $\alpha$  is the efficiency coefficient of the step attenuator.

The ENR values of the adjustable noise source were calculated using the output noise temperature ( $T_u$ ) in Eq. (6).

$$ENR(dB) = 10 \log \left( \frac{T_u - T_0}{T_0} \right), \quad (6)$$

where  $T_0$  is 290 K.

The outputs of the adjustable noise source, the standard noise source with 15 dB ENR, and the ambient source were measured in sequence, while the adjustable noise source value was changed in 1 dB steps. The noise temperatures were calculated using the measurement results from 12 to 18 GHz in Eq. (4) and the ENR values of the noise temperatures were calculated using Eq. (6).

The differences between the calculated and the measured ENR values from 4 to 15 dB varied between  $-0.22$  and  $0.48$  dB over all of the frequency ranges (Figure 6a). The obtained difference values were much larger than the desired ENR uncertainty, and so a polynomial fit was applied to the measured ENR values to reduce this difference. The graph of the difference between the calculated and corrected ENR values versus nominal

ENR values ranging from  $-0.08$  to  $0.10$  dB over all of the frequencies is shown in Figure 6b.

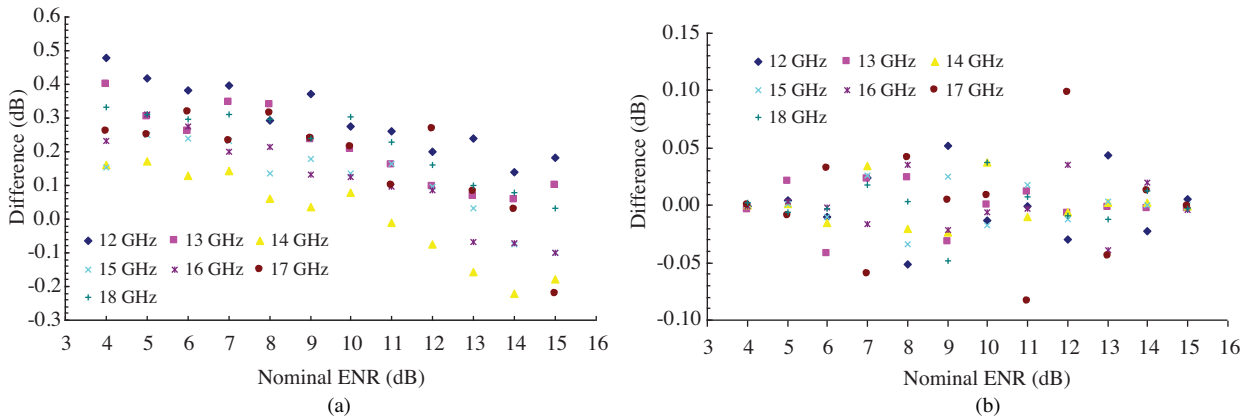


**Figure 6.** a) The difference between calculated and measured results. b) The difference between calculated and corrected results.

### 3.3. Experimental results

The radiometer’s performance was tested using 3 noise sources certified by the NPL and 1 noise source certified by its manufacturer. Two of them (model NC346C, NoiseCom Inc.) had a nominal 15 dB ENR, and the other 2 (model 346A, Hewlett-Packard) had a nominal 5 dB ENR. A 15 dB and a 5 dB noise source certified by the NPL were selected as standard noise sources, while the others were selected as unknown noise sources. The ENR values of each unknown noise source were measured using the set-up shown in Figure 2, without temperature control.

Certified and measured ENR values are compared in Figure 7, which shows data obtained using standard and unknown noise sources with nominal 15 dB ENR. The differences between the certified and the measured ENR values are shown in Figure 8, which shows data obtained using standard noise sources with nominal 15 dB and 5 dB ENR, and an unknown noise source with nominal 5 dB ENR. Changes in the accuracy and uncertainty

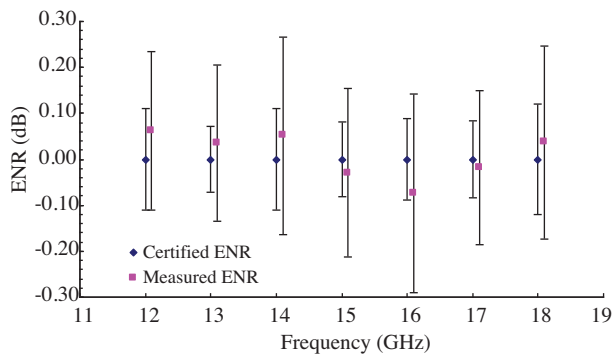


**Figure 7.** The differences between certified and measured ENR values of an unknown noise source with nominal 15 dB ENR.

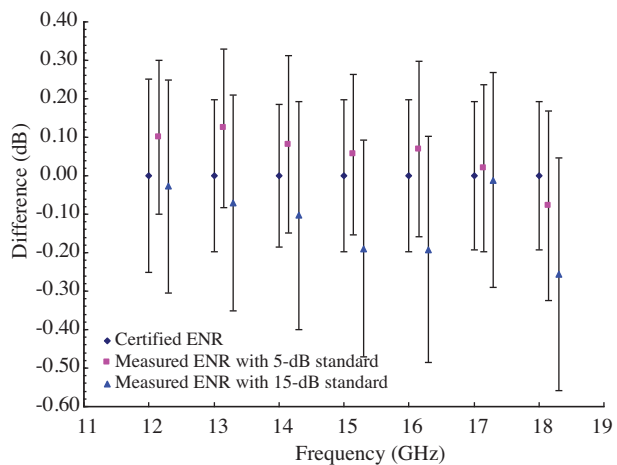


**Figure 8.** The differences between certified and measured ENR values of an unknown noise source with nominal 5 dB ENR.

of the results can be observed in Figures 7 and 8. Figure 7 demonstrates that the accuracy of the radiometer remained within the range of  $-0.07$  to  $0.06$  dB, and that the uncertainty varied between  $0.17$  and  $0.21$  dB.

When using the 5 dB unknown noise source, the accuracy of the radiometer remained within the range of  $-0.08$  to  $0.10$  dB for the 5 dB ENR standard, and the uncertainty varied from  $0.20$  to  $0.25$  dB, as shown in Figure 8.

Comparing the results of the 5 dB unknown noise source with those of the 15 dB standard noise source demonstrates that the accuracy of the radiometer varied from  $-0.26$  to  $0.01$  dB, and the uncertainty varied from  $0.28$  to  $0.30$  dB, as shown in Figure 8.

Nominally, equal-valued noise sources resulted in good measurement agreement. However, the use of nominally different sources resulted in larger measurement errors, and the linearity errors reached a maximum of approximately  $0.26$  dB.

## 4. Discussion

The expanded uncertainty of the noise source temperature,  $U(T_x)$ , can be calculated using Eq. (7), obtained from Eq. (4) [21].

$$U(T_x) = 2 \sqrt{\sum_{i=1}^n \left( \frac{\partial T_x}{\partial X_n} \right)^2 u^2(X_n)}, \quad (7)$$

where  $n$  is the number of the parameter in Eq. (4),  $X_n$  is the  $n$ th parameter,  $\frac{\partial T_x}{\partial X_n}$  is the sensitivity coefficient, and  $u(X_n)$  is the uncertainty of  $X_n$ . The uncertainties in the ENR values given in Figures 7 and 8 were calculated from Eqs. (4) and (7). The uncertainty budget for 18 GHz is presented in Table 2. Some calibration and measurement capabilities (CMCs) in coaxial lines on noise measurements of national metrology institutes (NMIs) declared in the Bureau International des Poids et Mesures (BIPM) database are given in Table 3 [22]. The uncertainty values of the developed radiometer are seen to be acceptable when compared to the uncertainties of the NMIs.

**Table 2.** Uncertainty budget of ENR measurement at 18 GHz.

Source of uncertainty	15 dB unknown 15 dB standard	5 dB unknown 5 dB standard	5 dB unknown 15 dB standard
Standard noise source (%)	1.56	1.19	1.11
Ambient noise source (%)	0.01	0.00	0.31
Standard - sw mismatch (%)	0.12	0.15	0.12
Unknown - sw mismatch (%)	0.15	0.14	0.14
Standard Y-factor (%)	0.86	1.26	0.71
Unknown Y-factor (%)	0.83	1.25	1.22
Standard - sw efficiency (%)	1.01	0.79	0.82
Unknown - sw efficiency (%)	1.00	0.77	0.75
Isolator (%)	0.10	0.02	0.10
Combined uncertainty ( $k = 1$ ) (%)	2.43	2.10	2.14
Expanded uncertainty ( $k = 2$ ) (%) (without linearity)	4.86	4.21	4.28
Linearity (dB)	0.00	0.00	0.10
ENR uncertainty ( $k = 2$ ) (dB)	0.21	0.25	0.30

**Table 3.** Some CMCs in the coaxial line on the noise measurements of NMIs published by the BIPM (values in parentheses were calculated from original values).

Metrology institute	Ranges	Expanded uncertainty (k = 2)
National Institute of Metrology (NIM), China	3.2 GHz-12.4 GHz 2 dB-20 dB	0.2 dB
Laboratoire National de Métrologie et d'essais (LNE), France	10 MHz-8.2 GHz 1000 K-100,000 K (3.89 dB-25.36 dB)	51 K-7171 K (0.22-0.30 dB)
National Metrology Institute of Japan (NMIJ)	2 GHz-18 GHz 150 K-12,000 K (up to 16.06 dB)	1.5%-3.7% (0.06-0.16 dB)
Korea Research Institute of Standards and Science (KRISS)	10 MHz-18 GHz 5 dB-17 dB	0.3 dB
Institute for Physical-Technical and Radiotechnical Measurements, Rostekhnregulirovaniye of Russia (VNIIFTRI)	1 GHz-18 GHz 77 K-100,000 K (up to 25.36 dB)	8 mK/K-16 mK/K (0.03-0.07 dB)
Federal Office of Metrology (METAS), Switzerland	10 MHz-26.5 GHz 5 dB-34 dB	0.15 dB-0.4 dB
Instituto Nacional de Técnica Aeroespacial (INTA), Spain	10 MHz-18 GHz 4 dB-16 dB	0.10 dB-0.29 dB
National Physical Laboratory (NPL), United Kingdom	10 MHz-18 GHz 77 K-100,000 K (up to 25.36 dB)	11 mK/K (0.05 dB)
National Institute of Standards and Technology (NIST), United States	12.4 GHz-18 GHz 10 K-15,000 K (up to 25.36 dB)	1.0%-1.2% (0.04dB-0.05 dB)

While considerable progress was made in linearity correction, it was too difficult to obtain the required linearity level in the comparison of different ENR values. Future work will be devoted to the further development of the WBCO attenuator, which will improve the linearity performance of the noise measurement system.

In order to minimize the temperature fluctuation of total power radiometers, 2 methods are used: active and passive temperature control. Active temperature control provides a constant defined temperature using complicated electronic systems. However, passive temperature control reduces the effects of instantaneous temperature fluctuation on the radiometer using huge thermal blocks. In this study, the 2 methods were compared, and the temperature fluctuation effects under passive temperature control were negligible because huge thermal blocks were used. Therefore, there was no need for active temperature control.

## 5. Conclusion

In this paper, we presented a total power radiometer developed to measure microwave noise temperature at frequency range from 12 to 18 GHz.

The radiometer was tested using 2 noise sources. The test results demonstrated that the radiometer has good output stability in time and temperature and does not require active temperature control. The temperature fluctuations of the developed radiometer remained below 4 mK for the required measurement time, and the obtained ENR values were in good agreement with their certified values.

Precise noise measurements at frequencies from 12 to 18 GHz can be performed using the radiometer established at the UME. Future work will be focused on the extension of the frequency range of the microwave total power radiometer from 50 MHz to 26.5 GHz.

## References

- [1] A. Einstein, "Investigations on the theory of the Brownian movement I (On the movement of small particles suspended in a stationary liquid demanded by the molecular-kinetic theory of heat)", *Annals of Physics*, Vol. 17, pp. 549-560, 1905.
- [2] J.B. Johnson, "Thermal agitation of electricity in conductors", *Physical Review*, Vol. 32, pp. 97-109, 1928.
- [3] H. Nyquist, "Thermal agitation of electric charge in conductors", *Physical Review*, Vol. 32, pp. 110-113, 1928.
- [4] R.H. Dicke, "The measurement of thermal radiation at microwave frequencies", *Review of Scientific Instruments*, Vol. 17, pp. 268-275, 1946.
- [5] A.J. Estlin, C.L. Trembath, J.S. Wells, W.J. Daywitt, "Absolute measurement of temperatures of microwave noise sources", *IRE Transactions on Instrumentation*, Vol. 9, pp. 209-213, 1960.
- [6] J.S. Wells, W.C. Daywitt, C.K.S. Miller, "Measurement of effective temperatures of microwave noise sources", *IEEE Transactions on Instrumentation and Measurement*, Vol. 13, pp. 17-28, 1964.
- [7] P.I. Somlo, D.L. Hollyway, "The Australian National Standards Laboratory X-band radiometer for the calibration of noise sources", *IEEE Transactions on Microwave and Techniques*, Vol. 16, pp. 664-666, 1968.
- [8] D.J. Blundell, E.W. Houghton, M.W. Sinclair, "Microwave noise standards in the United Kingdom", *IEEE Transactions on Instrumentation and Measurement*, Vol. 21, pp. 484-488, 1972.
- [9] M.S. Hersman, G.A. Gene, "Sensitivity of the total power radiometer with periodic absolute calibration", *IEEE Transactions on Microwave Theory and Techniques*, Vol. 29, pp. 32-40, 1981.
- [10] D.V. Land, A.P. Lewvick, J.W. Hand, "The use of the Allan deviation for the measurement of the noise and drift performance of microwave radiometers", *Measurement Science and Technologies*, Vol. 18, pp. 1917-1928, 2007.
- [11] S. Dia, B. Godara, F. Alicalapa, A. Fabre, "Ultra wide-band : state of the art; implementation of a performance-controllable low-noise amplifier", *Turkish Journal of Electrical Engineering & Computer Sciences*, Vol. 13, pp. 1-22, 2005.
- [12] F.T. Ulaby, R.K. Moore, A.K. Fung, *Microwave Remote Sensing: Active and Passive, Volume 1, Microwave Remote Sensing Fundamentals and Radiometry*, Norwood, Artech House, 1981.

- [13] J. Randa, D.K. Walker, "On-wafer measurement of transistor noise parameters at NIST", IEEE Transactions on Instrumentation and Measurement, Vol. 56, pp. 551-554, 2007.
- [14] S.P. Pucic, "Derivation of the system equation for null-balanced total-power radiometer system NCS1", Journal of Research of the National Institute of Standards and Technology, Vol. 99, pp. 55-63, 1994.
- [15] M.W. Sinclair, Microwave Measurements, London, Peter Peregrinus Ltd., 1989.
- [16] G. Evans, C.W. McLeish, RF Radiometer Handbook, Norwood, Artech House, 1977.
- [17] D.A. Thompson, R.L. Rogers, J.H. Davis, "Temperature compensation of total power radiometers", IEEE Transactions on Microwave Theory and Techniques, Vol. 51, pp. 2073-2078, 2003.
- [18] S.P. Pucic, "A null-balanced total-power radiometer system NCS1", Journal of Research of the National Institute of Standards and Technology, Vol. 99, pp. 45-53, 1994.
- [19] R. Swarup, J.R. Anand, P.S. Negi, "On 30 MHz TE<sub>11</sub> mode piston attenuator", Review of Scientific Instruments, Vol. 72, pp. 1858-1861, 2001.
- [20] C.K.S. Miller, W.C. Daywitt, M.G. Arthur, "Noise standards, measurements, and receiver noise definitions", Proceedings of the IEEE, Vol. 55, pp. 865-877, 1967.
- [21] P. Racette, R.H. Lang, "Radiometer design analysis based upon measurement uncertainty", Radio Science, Vol. 40, 2005.
- [22] Bureau International des Poids et Mesures (BIPM), Calibration and Measurement Capabilities, 2010. Available at [http://kcdb.bipm.org/appendixC/country\\_list.asp?Iservice=EM/RF.11.4.1](http://kcdb.bipm.org/appendixC/country_list.asp?Iservice=EM/RF.11.4.1).